의학박사 학위논문

Visualization of exosome-mediated miR-210 from hypoxic tumor cells

저산소 암세포 유래 miR-210 의 엑소좀을 통한 전달 영상화

2016 년 08 월

서울대학교 대학원

의과학과 의과학전공

정 경 오

A Thesis of the Degree of Doctor of Philosophy

저산소 암세포 유래 miR-210 의 엑소좀을 통한 전달 영상화

Visualization of exosome-mediated miR-210 from hypoxic tumor cells

August 2016

The Department of Biomedical Sciences
Seoul National University
College of Medicine

Kyung Oh Jung

저산소 암세포 유래 miR-210 의 엑소좀을 통한 전달 영상화

지도교수 정 준 기

의학 박사 학위논문으로 제출함
2016년 8월

서울대학교 대학원
의과학과 의과학전공
정 경 오

정경오의 의학박사 학위 논문을 인준함
2016년 8월

위 원 장 _____
부위원장 _____
위 원 _____
위 원 _____
위 원 _____

Visualization of exosome-mediated miR-210 from hypoxic tumor cells

by
Kyung Oh Jung

A thesis submitted to the Department of Biomedical Sciences
in partial fulfillment of the requirements
for the Degree of Doctor of Philosophy in Biomedical Sciences
at the Seoul National University College of Medicine

August, 2016

Approved by Thesis Committee:

Professor _____ **Chairman**
Professor _____ **Vice chairman**
Professor _____
Professor _____
Professor _____

ABSTRACT

Kyung Oh Jung
Department of Biomedical Sciences
The Graduate School
Seoul National University

Introduction: Cells release exosomes, which are known to carry specific cellular components such as proteins, mRNA, and miRNA for communicating with other cells. Particularly, cancer cells actively communicate with neighboring cancer cells and other cells in the tumor microenvironment. In this study, I constructed a DNA reporter gene vector to visualize miR-210 function, and established cell lines containing this construct. I transferred exosomes from hypoxic cancer cells into breast cancer cells and endothelial cells, and demonstrated the expression and function of miR-210 in the recipient cells.

Methods: To evaluate miR-210 function, I developed a miR-210 specific reporter (pCMV-luc2/miR-210), which was designed such that the luciferase signal was turned off on binding to miR-210. Using this vector, 4T1 (mouse

breast cancer cells) and SVEC (mouse endothelial cells) were transfected. Hypoxia was induced by Desferoximine (DFO). Hypoxic exosomes were isolated by ultracentrifugation or ExoQuick, and characterized by western blot analysis and transmission electron microscopy (TEM). Real-time PCR was performed to measure the amount of miR-210. Luciferase activity was measured by luciferase activity assay and IVIS imaging. In tumor tissues, immunohistochemistry was performed for detecting HIF-1a, luciferase, Ephrin-A3, PTP1B, and VEGF.

Results: The amount of miR-210 increased in hypoxic 4T1 cells, and in the exosomes from the hypoxic tumor cells. In bioluminescence imaging, luciferase signals of Exo (+) 4T1 and Exo (+) SVEC cells decreased, as compared to those of Exo (-) cells. In xenograft mouse models, the luciferase signals also decreased from tumors treated with hypoxic exosomes, indicating exosome-mediated transfer of miR-210. The expression of Ephrin-A3 and PTP1B, miR-210 target proteins also decreased in the hypoxic exosome-treated tumor cells, while the expression of VEGF increased.

Conclusion: Transfer of miR-210 through exosomes was successfully visualized from hypoxic cancer cells to cancer cells and endothelial cells, and had it had effects on angiogenesis-related genes. This imaging system can be

also applied to understand basic mechanism of intercellular communication between tumor microenvironment cells via exosomes.

Keywords: Breast cancer, exosome, hypoxia, miR-210, tumor microenvironment

Student number: 2010-23745

CONTENTS

LIST OF FIGURES AND TABLES

LIST OF ABBREVIATIONS

TEM, Transmission Electron Microscopy

GAA, Glutaraldehyde

RT-PCR, Reverse Transcription-Polymerase Chain Reaction

SDS, Sodium Dodecyl Sulfate

FBS, Fetal Bovine Serum

HBSS, Hank’s Balanced Salt Solution

DFO, Desferrioxamine

INTRODUCTION

Hypoxia is one of the important features in the tumor microenvironment that occurs due reduced supply of oxygen in cancer cells, and considered as a hallmark in cancer (1, 2). The interior cells become hypoxic with an abnormal increase in tumor mass, resulting in abnormal vascularization and uncontrolled cell proliferation. In these hypoxic tumors, HIF-1α is activated and induces various malignant phenotypes. HIF-1α, a subunit of a heterodimeric transcription factor, is considered the transcriptional regulator of developmental and cellular responses to hypoxia (3). The dysregulation of HIF-1α has adverse effects in cancer biology, including pathophysiology, cell survival, tumor invasion, vascularization, and angiogenesis (4). In addition, hypoxic tumors become resistant to chemotherapy and radiotherapy, making imaging of hypoxic cells important for cancer diagnosis and therapy (5, 6).

Many types of microRNAs (miRNAs) have recently been considered as biomarkers of cancers (7). miRNAs play important roles in regulating gene expression in cellular functions of many cancer types, including tumor progression, cellular differentiation, cell proliferation, and cell death. microRNAs are single-stranded, non-coding, small RNAs that regulate degradation or posttranslational inhibition of target mRNA by partially or completely binding to the 3′ untranslated

region (UTR) of that mRNA (8). Several studies have recently reported that miR-210 is highly upregulated in hypoxic cancer cells. miR-210 provides important roles in tumor formation, including angiogenesis (9, 10). Additionally, miR-210 is recently reported to affect the biological functions of endothelial cells such as cell survival, migration, angiogenesis, and differentiation (11).

To measure the level of miRNA expression, real-time PCR and northern blotting have been widely used as common detection methods (12,13). However, since these methods demand invasive procedures and some amount of tissues were needed for sample preparation, repeated sampling of miRNA is difficult. It is also difficult to evaluate the level of miRNA expression in vivo. Therefore, non-invasive imaging reporter systems were developed for monitoring miRNA which could be used in vivo (14). In this study, I used luciferase gene as a reporter gene for bioluminescent imaging and three copies of the complementary target sequences of miR-210 behind the luciferase gene. Luciferase signal-off system vector can be used to monitor the amount of miRNA by showing a decrease of luciferase signals in the presence of miRNA.

Molecular imaging using reporter genes has many advantages in field of biomedicine for diagnosis and therapy of cancer. In molecular biology, there are many reporter genes used in fluorescence imaging, bioluminescence imaging, MRI,

and nuclear medicine imaging, which could be applicable for in vivo models (15). Reporter gene imaging system could be used to visualize the expression levels of particular genes and various biologic phenomena. These systems also provide methods for visualizing tumor mass and monitoring the biodistributions of target cells, such as stem cells and immune cells, in vivo (16). Recently, as more efficient reporter gene systems have been developed, there are advances in the sensitivity and resolution of in vivo imaging. Therefore, molecular imaging using reporter genes play an important role in the diagnosis and therapy of cancer (17,18).

Exosomes are cell-derived extracellular vesicles with diameters ranging from 30 to 200 nm that were first described in the 1980s as organelles that remove cell debris. Recently, exosomes have received increased attention in medicine as diagnostic and therapeutic vesicles. They contain many functional proteins, lipids, mRNAs, and miRNAs, and are known to mediate intercellular communication in their microenvironment, acting as novel messengers in cell-to-cell communication (19, 20). Especially, exosomes derived from cancer cells have been reported to be transferred to tumor microenvironment cells, as well as surrounding tumor cells, where they become involved in tumor growth, immune suppression, apoptosis, invasion, angiogenesis, and metastasis (21-23).

A recent study revealed that hypoxic cancer cells secreted relatively increased number of exosomes, along with an increase in their miR-210 content (24, 25). However, the transfer and effects of exosomal miR-210 in various recipient cells have not been investigated.

The aim of this study

In this study, I constructed a DNA reporter gene vector to visualize miR-210 function, and established cell lines (breast cancer cells and endothelial cells) containing this construct. I transferred exosomes from hypoxic cancer cells into breast cancer cells and endothelial cells, and demonstrated the expression and function of miR-210 in the recipient cells.

MATERIAL AND METHODS

Establishment of stable cell lines and hypoxic exposure

The mouse breast cancer cell line 4T1 and mouse endothelial cells SVEC were cultured as monolayers in Roswell Park Memorial Institute (RPMI) 1640 medium supplemented with 1% antibiotic–antimycotic mix and 10% fetal bovine serum (FBS). SVEC and 4T1 cells were then infected by retroviruses with reporter gene vectors pCMV-luc2/miR-210, whose luciferase signal could be turned off by binding of miR-210 to any of the three miR-210 binding sites at the 3' end of luciferase. Stable cell lines were selected by treatment with puromycin (2 g/mL) for 2 weeks. We labeled 4T1 cell lines with pCMV-luc2/miR-210 to 4T1-luc2/miR-210. Hypoxia was induced with Desferrioxamine (DFO) (Sigma-Aldrich, St Louis, MO, USA) at 37℃ in a 5% CO_2 humidified environment.

Exosome purification

The 4T1 cells (1×10^6) were cultured in a conditioned medium. After 48 h, exosomes were isolated from the cultured medium, using an ultracentrifuge (10,000 × *g*) and an exosome purification kit ExoQuickTM (System Bioscience, Mountain View, CA, USA). The exosome pellets were washed and resuspended in PBS. Proteins from exosome pellets and lysed cells were obtained using 1X RIPA

buffer (25 mM Tris-HCl pH 7.6, 150 mM NaCl, 1% NP-40, 1% sodium deoxycholate, 0.1% SDS) with a cocktail of anti-proteases (Roche, Nutley, NJ, USA). Protein concentrations in exosome pellets and cell lysates were measured using a BCA Protein Assay Kit (Pierce, Rockford, IL, USA). The amounts of exosomes under normoxic and hypoxic conditions were compared from the protein concentrations.

Western blotting

Proteins (20 μg) in exosome pellets and cell lysates were separated using bis-Tris-HCl-buffered 4%–12% gradient polyacrylamide gels (Invitrogen, Carlsbad, CA, USA), and blotted onto PVDF membranes (Millipore, Watford, UK). The membrane was blocked with 3% skim milk in TBS-T (20 mM Tris, 0.1% Tween 20, and 137 mM NaCl) at room temperature for 1 hour. Next, the membrane was treated with primary antibodies overnight at 4℃ as follows: anti-AIP1/Alix (1:250 dilution; BD Biosciences, San Jose, CA, USA), anti-CD63 (1:500 dilution; System Bioscience, Mountain View, CA, USA), anti-CD9 (1:500; System Bioscience, Mountain View, CA, USA), and anti-calnexin (1:500; Santa Crux Biotechnology, Santa Cruz, CA, USA). The membrane was then incubated with secondary antibodies at room temperature for 1 hour after washing 3 times with TBS-T. The

secondary antibodies were used as follows: anti-mouse for AIP1/Alix (1:2,000 dilution, Invitrogen-Molecular Probes, Eugene, Oregon), anti-rabbit for CD63 and CD9 (1:2,000 dilution, System Bioscience, Mountain View, CA, USA) and anti-goat for calnexin (1:2,000 dilution, Invitrogen-Molecular Probes, Eugene, Oregon). Western blot was visualized using ECL reagents (Roche, Nutley, NJ, USA), and imaged by LAS-3000 imaging system (Fuji Film, Tokyo, Japan).

Transmission Electron Microscopy (TEM) and nanosight

The exosome pellets were fixed with 2% glutaraldehyde (GAA) overnight at 4℃. The samples were deposited by a copper grid (300 mesh and covered with carbon), and the exosome size was analyzed using TEM images obtained by JEOL (JEM 1400) transmission electron microscope at 80 keV and Nanosight.

Fluorescent exosome imaging *in vitro*

A stock solution of the lipophilic tracer DiO and DiI (Invitrogen, Carlsbad, CA, USA) was prepared in ethanol and DMSO. Exosomes isolated from cultured medium-derived 4T1 cells were incubated with DiO and DiI (1 μM) for 30 minutes at 37℃. The exosomes were washed with PBS and purified using ExoQuick^{TM}. The fluorescent-labeled exosomes (20 μg/mL) were treated in tumor cells; 4T1,

endothelial cells; SVEC, macrophage; Raw264.7, stem cells; mBM-MSC (Primary cells isolated from Balb/c bone marrow), fibroblast; 3T3, and dendritic cells; JAWS2. Fluorescence of exosomes in cells was detected using the Zeiss LSM510 META confocal imaging system (Carl Zeiss, Thornwood, CA, USA). We also constructed a CMV driven RFP- tagged CD9 vector, and imaged exosomes using confocal microscopy.

Cell viability assay

To evaluate the cytotoxicity of DFO and exosomes in 4T1 and SVEC cells, cell viability assays were performed 48 h after dose-dependent DFO (0 μM, 200 μM, 400 μM, and 800 μM) and exosome (0 μg/mL, 200 μg/mL, 400 μg/mL, and 800 μg/mL) treatments. The cells were treated with Cell Counting Kit-8 (CCK-8) solution, and after incubation for 2 h, the mean value of the OD at 450 nm was measured.

Effects of hypoxic exosomes in SVEC cells

To confirm the effects of hypoxic exosomes, SVEC cells were treated with hypoxic exosomes from 4T1 cells (400 μg/mL) for 48 h. Wound healing assay and

capillary-like structures were confirmed using microscopy. Proliferation was also confirmed by Cell Counting Kit-8 (CCK-8) solution.

Fluorescence labeling of exosomes for in vivo use

To label exosomes with Cy7, 50 μg of exosome in a total volume of 100 μl was mixed with 0.5 μg of CyTM7 monoNHS ester (5 μM, Amersham Biosciences) for 10 min at 37 ℃. ExoQuickTM was used to purify Cy7-labeled exosomes, followed by centrifugation at 3,000g for 15 min.

Tumor xenografts in nude mice

All procedures involving *in vivo* mice studies were approved by the Institutional Animal Care and Use Committee at Seoul National University, and were consistent with the Guide for the Care and Use of Laboratory Animals. 4T1-luc2/miR210 cells (1×10^6) were subcutaneously transplanted in the thigh of a 6-week-old male BALB/c nu/nu mouse weighing 20 g on average, and the tumors were grown to 10 mm in diameter.

***In vivo* fluorescence imaging**

Cy7 labeled exosomes were intravenously injected in tumor xenograft of a mouse. The signals of exosomes were imaged by IVIS200 imaging system (Xenogen Corp., Alameda, CA, USA) equipped with a CCD camera.

Quantification of miR-210 by RT-qPCR

The 4T1 cells (1×10^6) were cultured in a conditioned medium, and then treated with 400 μM DFO for 48 h. Mouse blood in tumor xenografts was collected by cardiac puncture 48 h after 400 μM DFO treatment, and exosomes were isolated from the blood. Total RNA was extracted from cells and isolated exosomes into culture medium and blood, using TRIzol reagent (Invitrogen, Carlsbad, CA, USA). Quantification of miR-210 in hypoxic cells and exosomes was performed using SYBR Green Real time PCR Master Mix and Mir-X™ miRNA First-Strand Synthesis (TaKaRa, Otsu, Japan), according to the manufacturer's instructions. U6 was used as a housekeeping gene to standardize the initial miRNAs of a sample. The following formula gives relative values of gene expression, and the data were presented as either fold downregulation or upregulation:

fold value = $2^{-\Delta\Delta Ct}$,

where ΔΔCt = (Ct of gene of interest, treated-Ct of housekeeping gene, treated) - (Ct of gene of interest, control-Ct of housekeeping gene, control)

and Ct is the threshold cycle number.

The sequences of the primer were as follows:

miR-210 forward 5'-CTGTGCGTGTGACAGCGGCTGA -3',

HIF-1α forward 5'-GCACAGGCCACATTCACG-3', and

U6 forward 5'-TGGCCCCTGCGCAAGGATG -3'.

In vitro imaging of miR-210 activation induced by DFO and exosomes

The 4T1-luc2/miR210 cells (1×10^5) were seeded in 24 well plates. The cells were treated with DFO (400 μM), or exosomes (400 μg) isolated from cells treated with DFO (400 μM). After 48 h, the cells were treated with 100 ul of Luc substrate luciferin (0.3 μg/μl) followed by bioluminescence imaging. The imaging was done using the IVIS200 imaging system equipped with a CCD camera (Xenogen Corp., Alameda, CA, USA). Bioluminescent color images were analyzed using LIVINGIMAGE V. 2.50.1 software (Xenogen Corp., Alameda, CA, USA).

In vitro luciferase assays

Bioluminescence assays were performed using Luciferase Assay Kits (Applied Biosystems, Carlsbad, CA, USA). The cells were plated and treated with DFO or exosome, as described previously. After 48 h, the wells were washed twice with

PBS, and lysis solution was added to each well. The cell lysates were then transferred to a microplate. Bioluminescence intensities were measured using a Wallac 1420 VICTOR3 V (PerkinElmer Life and Analytical Sciences, Shelton, CT, USA).

***In vivo* imaging of miR-210 activation induced by DFO and exosomes**

In the DFO-treated group, mice were injected intratumorally with PBS in the left thigh and DFO (400 μM) in the right thigh. In the exosomes treatment group, mice were injected intratumorally with PBS in the left thigh and exosomes (400 μg/mL) in the right. After 48 h, the mice were intraperitoneally injected with 100 ul of Luc substrate luciferin (30 μg/μl), 10 min prior to bioluminescence imaging. Mice were anesthetized with isoflurane, and the imaging was performed in the IVIS200 imaging system, as described previously.

Immunohistochemistry (IHC)

IHC study was performed to compare the expression of luciferase, HIF-1α, and miR-210 target gene, Ephrin-A3, in tumors treated with either DFO or exosomes. Tumor tissues were fixed in 3.7% paraformaldehyde for 24 h. After paraffin embedding, 4 μm sections were sliced serially and mounted on a slide. The antigen

retrieval method was applied by boiling the tissues in citrate buffer (DakoCytomation, Glostrup, Denmark) for 5 minutes. Next, the tissues were treated with primary antibodies overnight at 4℃ as follows: anti-luciferase (1:500; Abcam, Cambridge, UK), anti-HIF-1α (1:100; Novus Biologicals, Littleton, CO, USA), and anti-Ephrin-A3 (1:500; Santa Crux Biotechnology, Santa Cruz, CA, USA). The secondary antibodies used are as follows: biotinylated anti-goat for luciferase (1:500; Dako, Glostrup, Denmark), and biotinylated anti-mouse for HIF-1α and Ephrin-A3 (1:500; Dako, Glostrup, Denmark). The samples were amplified with a complex of avidin-biotin peroxidase, and developed using DAB. Then, samples were counterstained with hematoxylin.

Western blot from FFPE tissue

Proteins (50 μg) extracted from FFPE tissues were separated as mentioned above. The primary antibodies were treated overnight at 4℃ as follows: anti-Ephrin-A3 (1:50 dilution; Santa Crux Biotechnology, Santa Cruz, CA, USA), anti-PTP1B (1:200 dilution; Abcam, Cambridge, UK), and anti-VEGF (1:200 dilution; Abcam, Cambridge, UK). The secondary antibodies were used as follows: anti-rabbit for Ephrin-A3, PTP1B, and VEGF (1:2,000 dilution, Cell signaling Technology, Danvers, MA, USA). Beta-actin was used as a housekeeping gene standard.

Statistical analysis

All results were presented as means ± SD. The t-test was used to determine the statistical significances, and p-values < 0.05 were considered statistically significant.

RESULTS

Characterization of exosome in a hypoxic environment

After purification of exosomes in a conditioned medium, the purified exosomes were characterized. TEM imaging and nanosight results revealed the presence of microvesicles within the expected size range for exosomes (about 100 nm), as shown in Figs. 1a and b. Western blot was performed using antibody of exosome marker proteins such as CD9, CD63, and Alix, and antibody of cell marker protein such as calnexin (Fig. 1c). The results showed that more exosome marker proteins expressed in exosomes than in cells, while more cell marker proteins expressed in cells than in exosomes. To examine the impacts of hypoxia on exosomes, 4T1 cells were cultured in a medium with (+) or without (-) DFO. The cells cultured in DFO (+) medium demonstrated significantly higher exosome concentrations (1.40±0.14 fold, $p = 0.0047$), as compared to those cultured in DFO (-) medium (Fig. 2a). In RT-PCR, mRNA of HIF-1α was increased in DFO (+) cells, as compared to DFO (-) cells, while there was no mRNA in DFO (+) and DFO (-) exosomes (Fig. 2b). In the western blot, protein content of HIF-1α was higher in DFO (+) cells, as compared to DFO (-) cells. Protein content of HIF-1α was also higher in DFO (+) exosomes, as compared to DFO (-) exosomes (Fig. 2c).

To evaluate the induction of hypoxia by DFO treatment, the levels of HIF-1α and miR-210 were compared in DFO (-) and DFO (+) cells using real-time PCR. Fig. 3a shows the increased expression levels of cellular HIF-1α (2.73±0.27 fold) in DFO (+) cells , as compared with those of the DFO (-) cells. However, there was no significant difference in the HIF-1α expression levels in DFO (-) and DFO (+) exosomes. For miR-210 (Fig. 3b), the levels of cellular miR-210 in DFO (+) cells demonstrated a significant increase, as compared with those of DFO (-) cells (15.70±5.84 fold; P = 0. 0184). The levels of exosomal miR-210 in DFO (+) exosomes were significantly increased in comparison with those of DFO (-) exosomes (12.73±3.59 fold; P = 0. 0023). These results suggest that hypoxia could be induced in 4T1 cells by DFO treatment, and exosome release and exosomal miR-210 could be enhanced by hypoxic condition.

To confirm miR-210 transfer through exosome in hypoxic tumor mouse blood, exosomes were isolated from mouse blood (Fig. 4a). Real-time PCR for miR-210 (Fig. 4b) showed that the levels of exosomal miR-210 in DFO (+) mouse serum were significantly higher than those in DFO (-) mouse serum (3.71±0.71 fold; P = 0.0368). These results suggest that hypoxia induced miR-210 could be transferred by exosomes, which could be further accumulated in tumor cells. To evaluate their accumulation in tumor, exosomes were labeled with a fluorescence

dye, Cy7, and imaged by IVIS after intravenous injection. Pellets of Cy7-exosomes were imaged by the Maestro™ *in vivo* fluorescence imaging system (Fig. 5a). Cy7-exosomes were intravenously injected in 4T1 xenograft model. IVIS images showed accumulation of Cy7-exosomes in 4T1 tumor *in vivo* (Fig. 5b) and *ex vivo* (Fig. 5c).

a) **Ultracentrifuge** **ExoQuick**

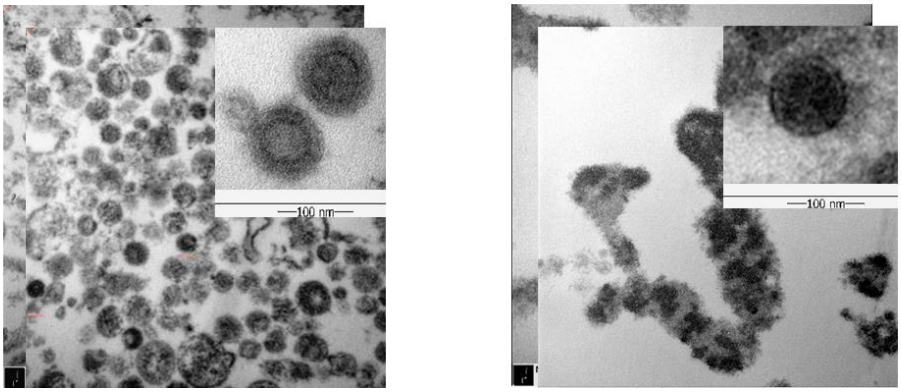

b)

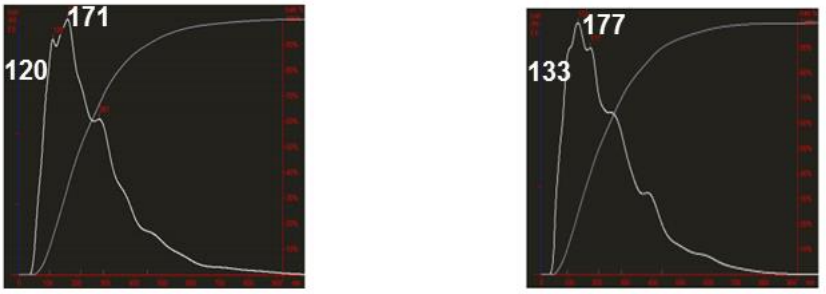

Particle Size / Concentration Particle Size / Concentration

c)

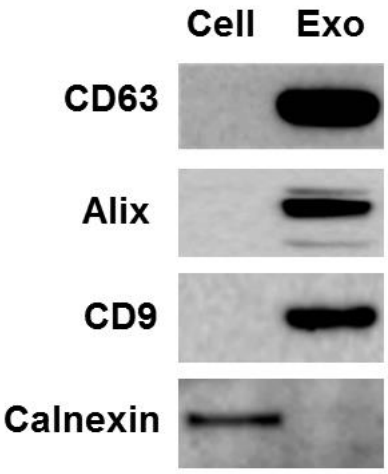

Figure 1. Isolation and characterization of exosome.

Exosomes were purified from the cultured medium by ultracentrifugation and ExoQuick™. (a and b) Exosome sizes were confirmed at ~100 nm by TEM imaging and NanoSight. (c) In western blot analysis, as expected, exosome marker proteins such CD9, CD63, and Alix were expressed in exosomes, and cell marker protein such as calnexin was expressed in cells. For induction of hypoxia, 4T1 cells with DFO (400 μM) were incubated for 48 h.

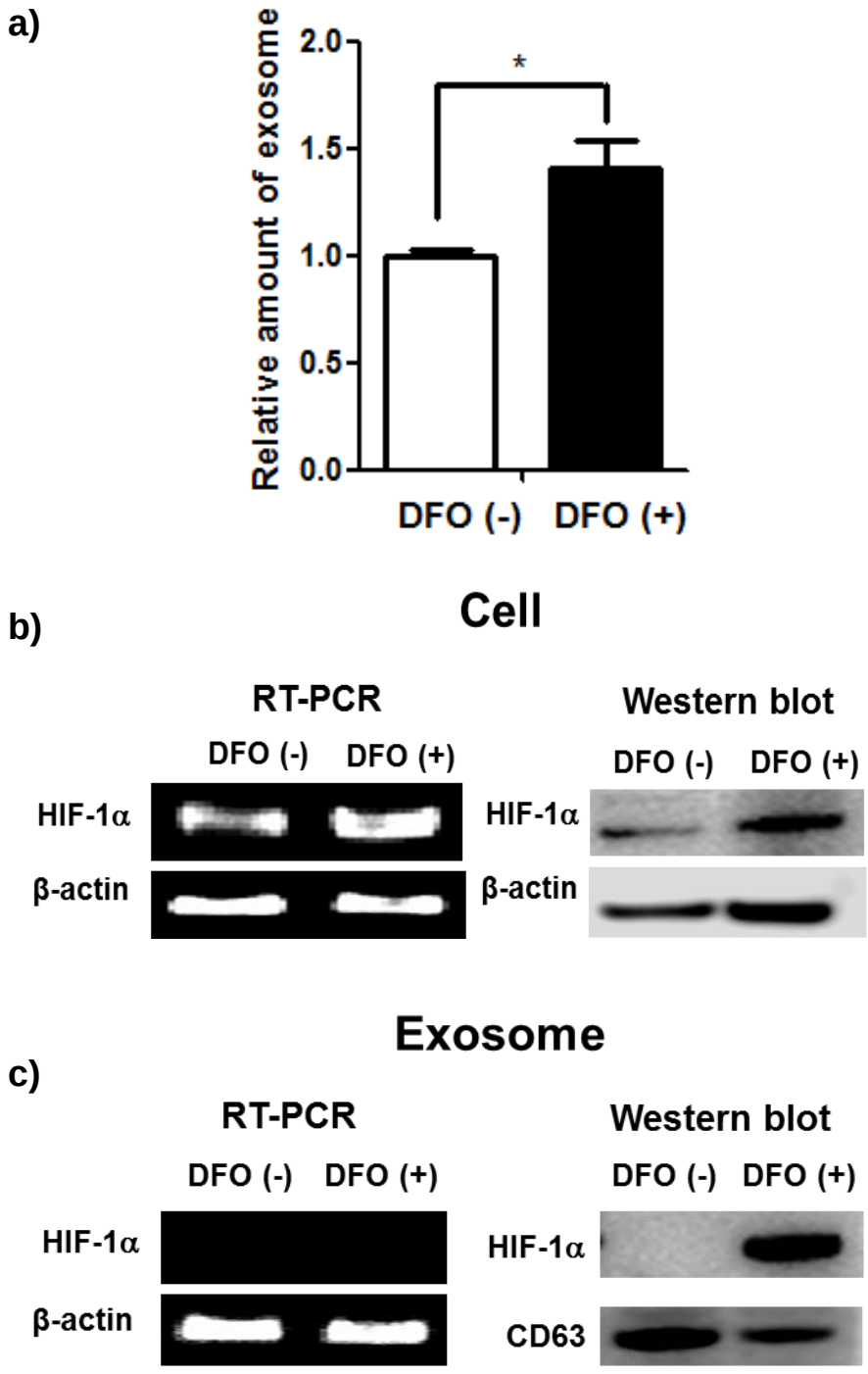

Figure 2. 4T1 cells and exosomes in a hypoxic environment.

To confirm the induction of a hypoxic environment by DFO, the concentration of exosomes was evaluated using a protein assay. (a) The concentration of DFO (+) exosomes was significantly higher, 1.40±0.14 fold, compared to that of DFO (-) exosomes. (b) RT-PCR showed that mRNA of HIF-1α was higher in DFO (+) cells compared to DFO (-) cells, while there was HIF-1α mRNA in DFO (+) and DFO (-) exosomes. (c) Western blotting showed that HIF-1α protein was increased in DFO (+) cells compared to DFO (-) cells, as well as in exosomes.

a) Realtime PCR for HIF-1α

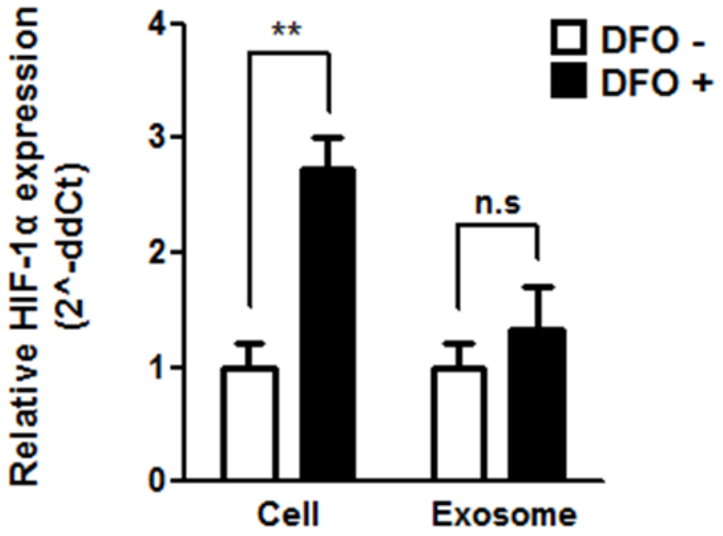

b) Realtime PCR for miR-210

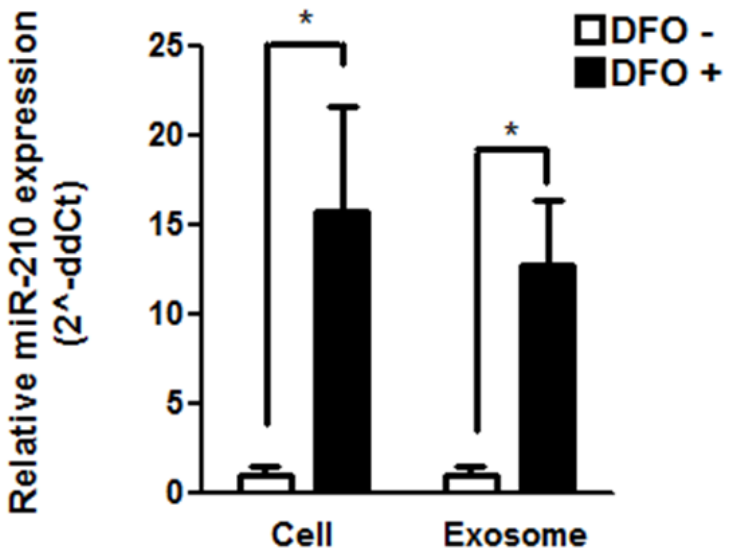

Figure 3. Expression of miR-210 and HIF-1α in hypoxic cells or hypoxic exosomes.

(a) Real-time PCR analysis showed that the levels of HIF-1α in DFO (+) cells were significantly higher, 2.73 ± 0.27 fold, as compared to those in DFO (-) cells, while there was no significant change in their expression levels in exosomes. (b) The levels of miR-210 in DFO (+) cells were significantly increased, 15.70±5.84 fold, as compared to those of DFO (-) cells, and the levels of miR-210 in DFO (+) exosomes also significantly increased, by 12.73±3.89 fold, as compared to those of DFO (-) exosomes. *statistical significance with p values <0.05.

a) Control group DFO treat group

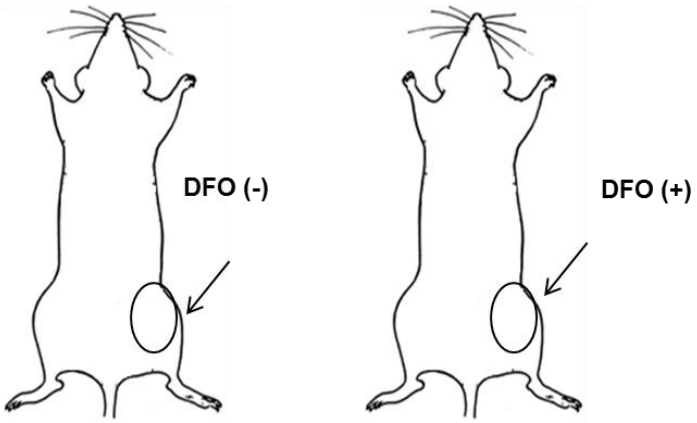

Mouse serum Exosome

b)

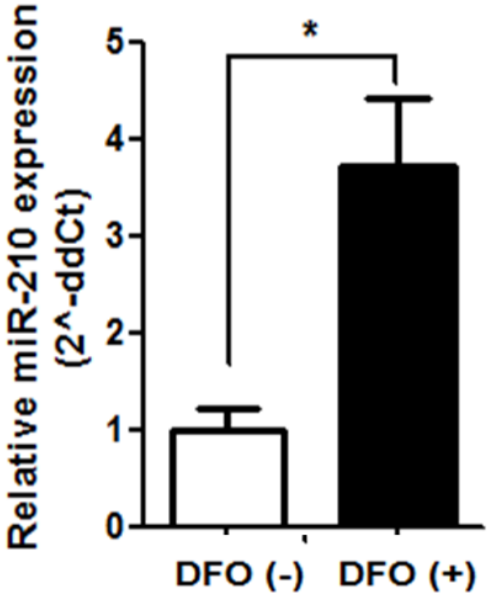

Figure 4. Hypoxic response of tumor in animal models.

(a) Exosomal miR-210 was purified from mouse serum. (b) Exosomal miR-210 levels of DFO (+) mouse serum were increased significantly (3.71±0.71 fold), as compared to those of DFO (-) mouse serum. *statistical significance with p values <0.05.

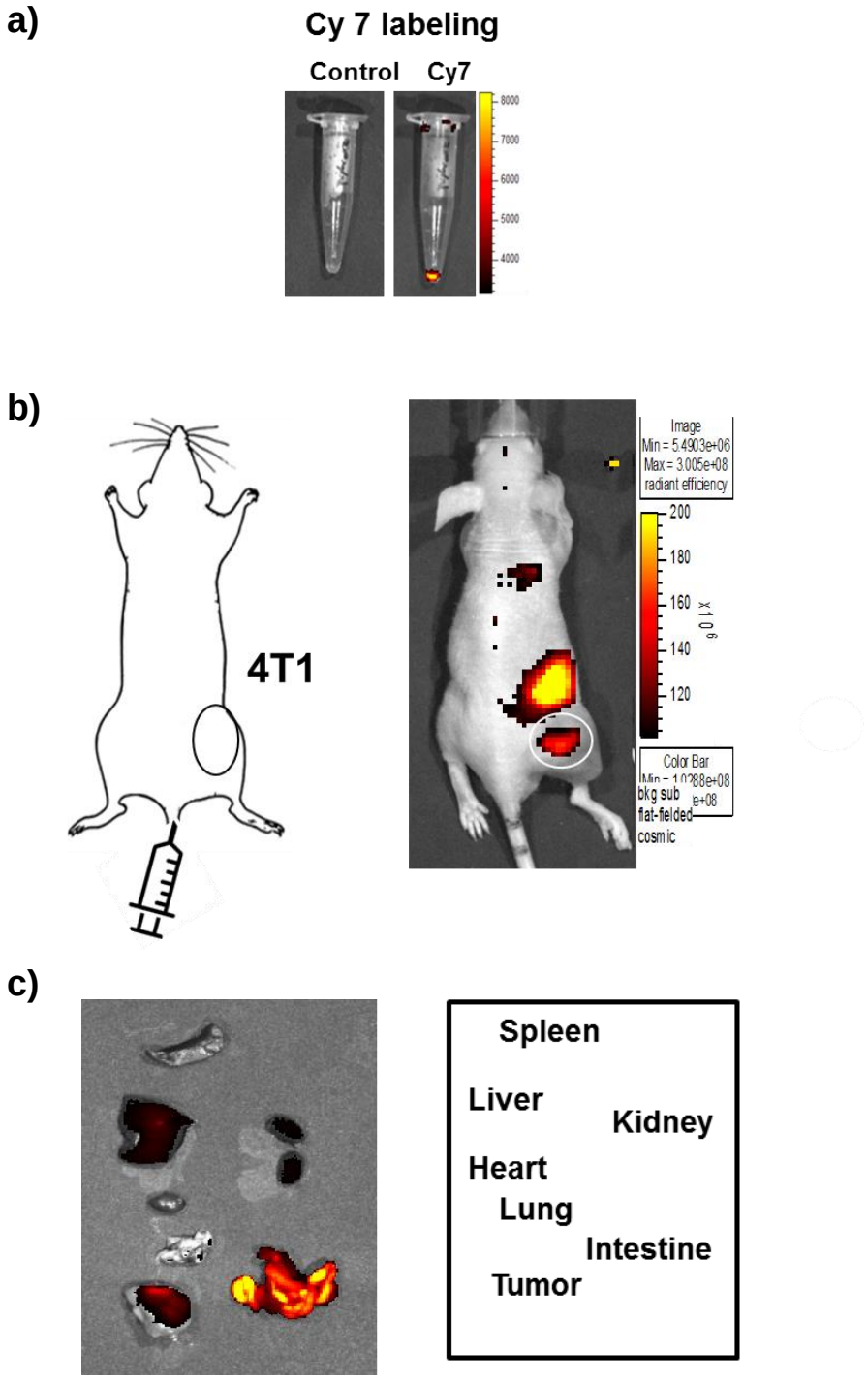

Figure 5. Exosome uptake imaging of tumor in animal model.

(a) Pellet of exosomes was imaged by IVIS. IVIS images showed Cy7 signals of 4T1 tumors (b) *in vivo* and (c) *ex vivo*.

Imaging of miR-210 activation in hypoxic cancer cells.

We established 4T1-luc2/miR-210 cells, in which the luciferase signal could be turned off by binding with miR-210 (Fig. 6). To confirm the vector function, miR-210 was induced by DFO treatment (0 μM, 10 μM, 100 μM, 200 μM, and 400 μM), and evaluated using bioluminescence imaging and luciferase assay. IVIS images (Fig. 7a and 7b) showed that the luciferase signal decreased in a dose dependent manner. Luciferase assay also showed a dose dependent decrease of luciferase activity (Fig. 7c). In bioluminescence imaging of cells, luciferase signals of DFO (+) cells (400 μM) decreased, as compared to that of DFO (-) cells (Fig. 8a). From ROIs of DFO (-) and DFO (+) cells, signals of DFO (+) cells were significantly decreased by 0.22±0.03 fold, as compared to those of DFO (-) cells (P = 0. 0057). In bioluminescence imaging of mice models (Fig. 8b), luciferase signals of DFO (+) tumor were also decreased after DFO treatment, whereas signals of DFO (-) tumor remained consistent pre- and post-treatment. From ROIs, signals of DFO (+) tumor were significantly decreased (0.53±0.07 fold, p = 0. 0271), whereas signals of DFO (-) tumor did not decrease significantly. In the extracted tissues (Fig. 8c), luciferase expression in DFO (+) tumor was decreased, as compared to that in DFO (-) tumor, while HIF-1α expression in DFO (+) tumor was increased, as compared to that in DFO (-) tumor. These results showed that

luciferase signal-off vector system for imaging miR-210 functions well *in vitro* and in vivo.

Figure 6. miR-210 reporter gene vector construct.

To image miR-210 activation, 4T1-luc2/miR-210 cells were constructed with a switch system vector in which luciferase signals could be turned off by the binding of miR-210. Hypoxia was induced by DFO treatment in medium for *in vitro* studies and intratumoral injection for *in vivo* studies, respectively. The miR-210 reporter construct is illustrated.

a)

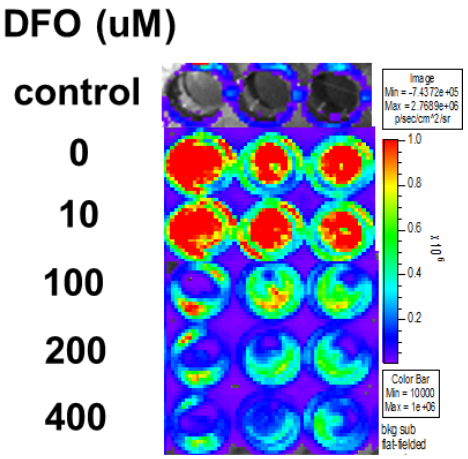
DFO (uM)
control
0
10
100
200
400
Image
Min = -7.4372e+05
Max = 2.7689e+06
p/sec/cm^2/sr
1.0
0.8
0.6
0.4
0.2
x 10^6
Color Bar
Min = 10000
Max = 1e+06
bkg sub
flat-fielded

b)

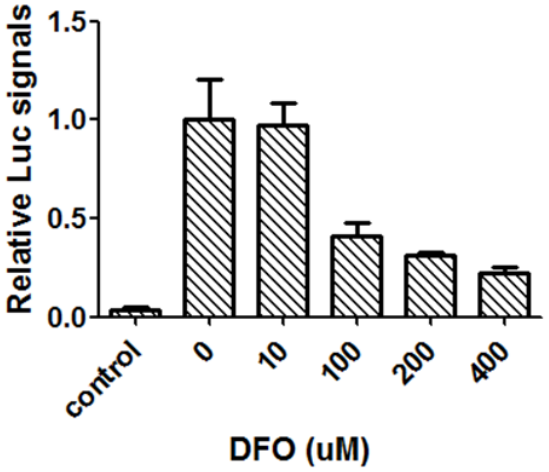
Relative Luc signals
1.5
1.0
0.5
0.0
control
0
10
100
200
400
DFO (uM)

c)

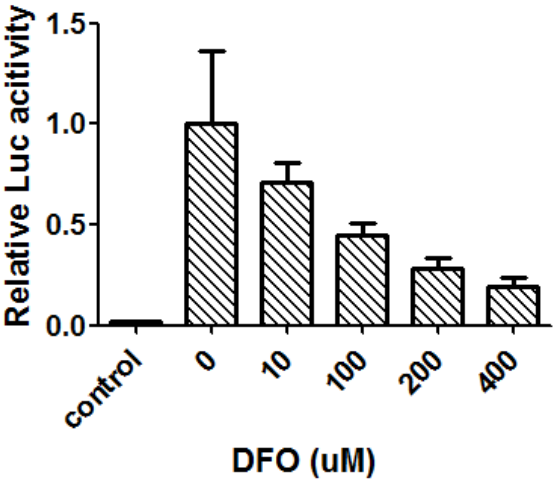
Relative Luc acitivity
1.5
1.0
0.5
0.0
control
0
10
100
200
400
DFO (uM)

Figure 7. Imaging for miR-210 activation induced by hypoxia in 4T1 cells.

DFO was treated in a dose-dependent manners (0 μM, 10 μM, 100 μM, 200 μM, and 400 μM). (a and b) IVIS images and luciferase assays showed that the luciferase signals, and (c) the luciferase activity decreased in a dose-dependent manner. Bioluminescence imaging showed that luciferase (Luc) signals of DFO (+) cells were significantly decreased, 0.22±0.03 fold, compared to those of DFO (-) cells at 48 h after DFO treatment (400 μM).

a)

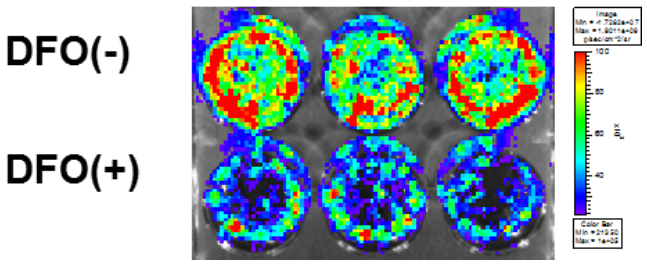

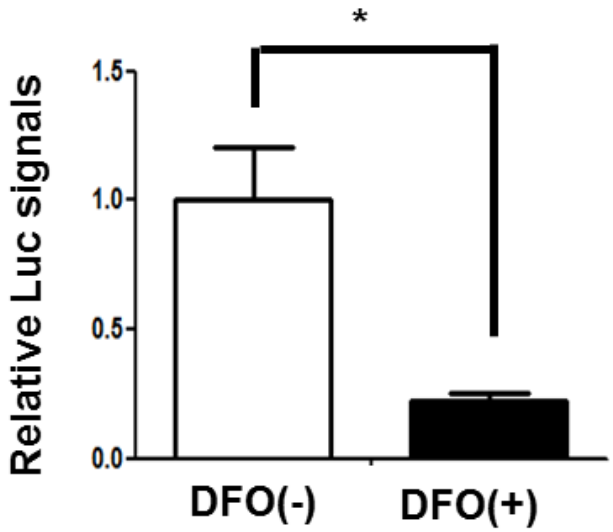

b)

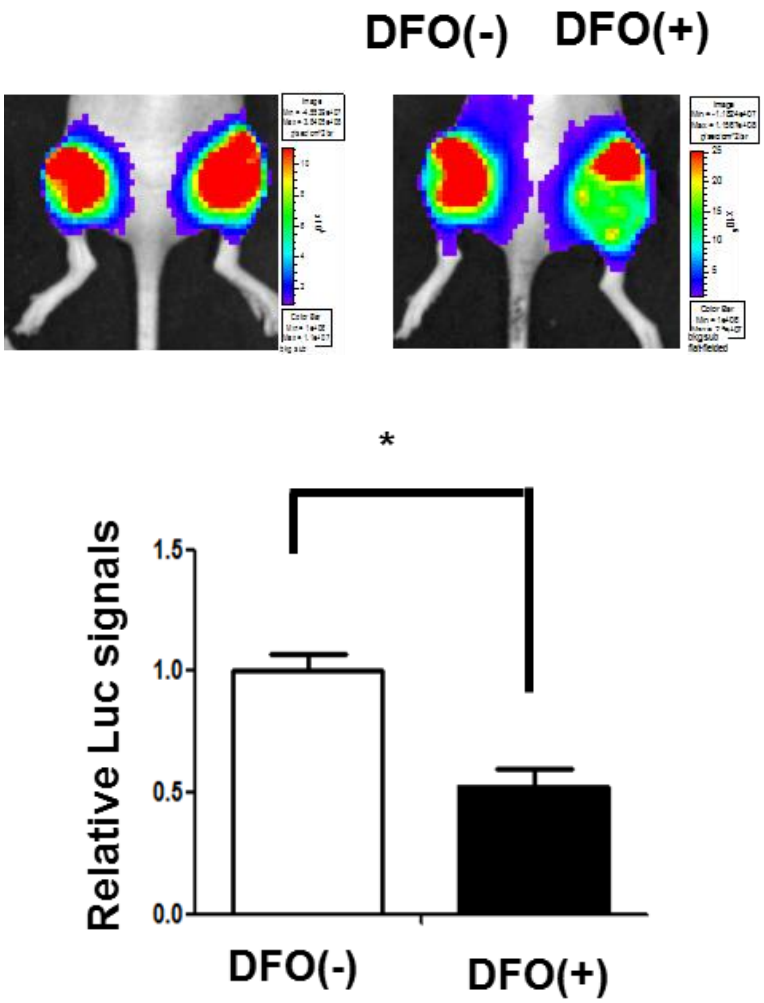

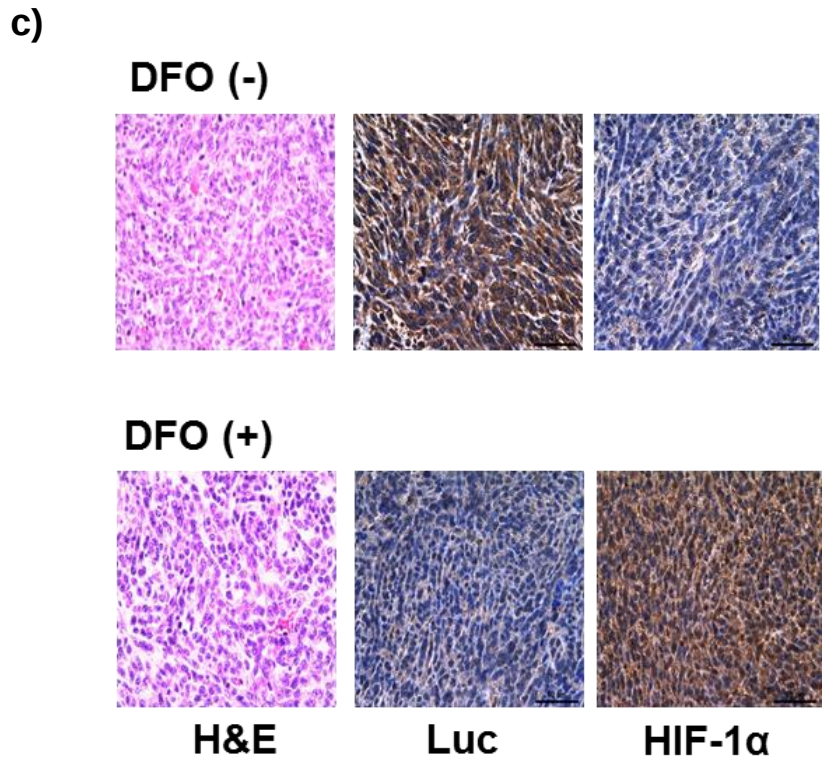

Figure 8. Imaging for miR-210 activation induced by hypoxia in animal models and ex vivo tissues.

(a) In bioluminescence imaging of cells, luciferase signals of DFO (+) cells were significantly decreased by 0.22±0.03 fold, compared to those of DFO (-) cells. (b) In bioluminescence imaging of mice, luciferase signals of DFO (+) tumor also decreased significantly, 0.53±0.07 fold, 48 h after DFO treatment, whereas signals of DFO (-) tumors did not decrease significantly (n = 3). (c) In tissues, luciferase expression in DFO (+) tumors decreased, as compared to that in DFO (-) tumors, whereas HIF-1α expression in DFO (+) tumors increased, as compared to that in DFO (-) tumors. *statistical significance with p values <0.05.

***In vitro* exosome imaging in tumor microenvironmental cells**

To confirm exosome uptake in tumor microenvironmental cells, exosomes labeled with DiI (red fluorescence; Ex565nm, Em594nm) and DiO (green fluorescence; Ex484nm, Em501nm) were imaged using confocal microscopy (Fig 9a) and live cell imaging (Fig 9b). These fluorescent-labeled exosomes (20 μg/mL) were treated in various cells such as tumor cells; 4T1, endothelial cells; SVEC, macrophage; Raw264.7 (Fig 10a), stem cells; mBs-MSC, fibroblast; 3T3, and dentritic cells; JAWS2 (Fig 10b). Using a fluorescent dye and a confocal microscope, uptake of exosomes was imaged in various cells. To image exosomes by another method (Fig 9c), we constructed CMV driven RFP- tagged CD9 vector, wherein CD9, a well-known exosomal marker protein, is tagged with red fluorescent protein (RFP). In confocal microscopy, 4T1 cells were transfected by CD9/RFP vector and exosomes inside 4T1 cells were imaged. These results demonstrated that exosomes from cultured medium were labeled with a fluorescent dye, and fluorescent exosomes were taken up and migrated to 4T1 cells.

a)

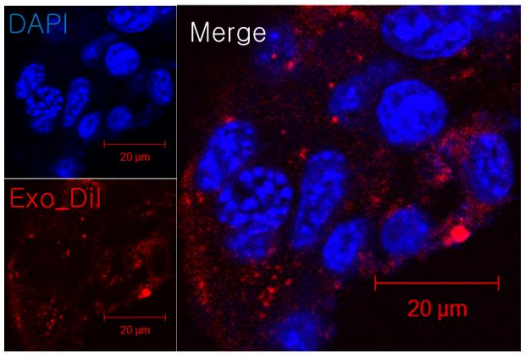

b)

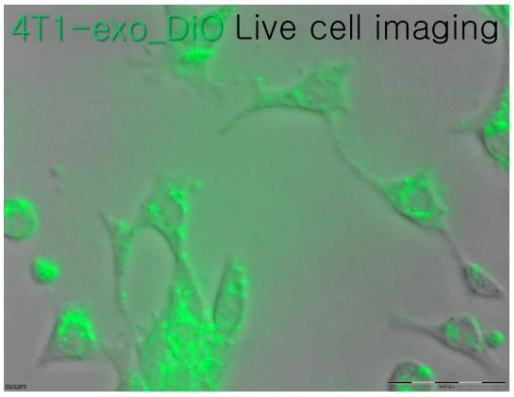

c)

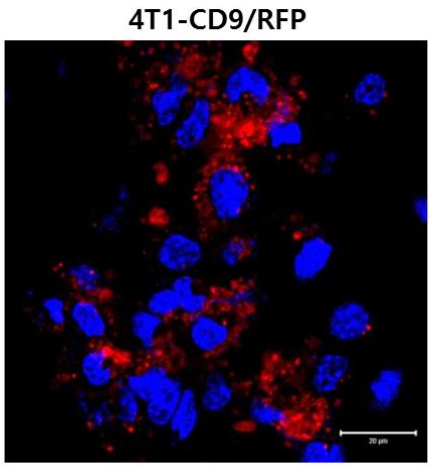

Figure 9. Exosome uptake images using fluorescence imaging.

Exosomes labeled with DiI and DiO were imaged by (a) confocal microscopy and (b) live cell imaging. (c) As another imaging method for exosomes, 4T1 cells were transfected by CD9/RFP vector and exosomes inside 4T1 cells were imaged in confocal microscopy.

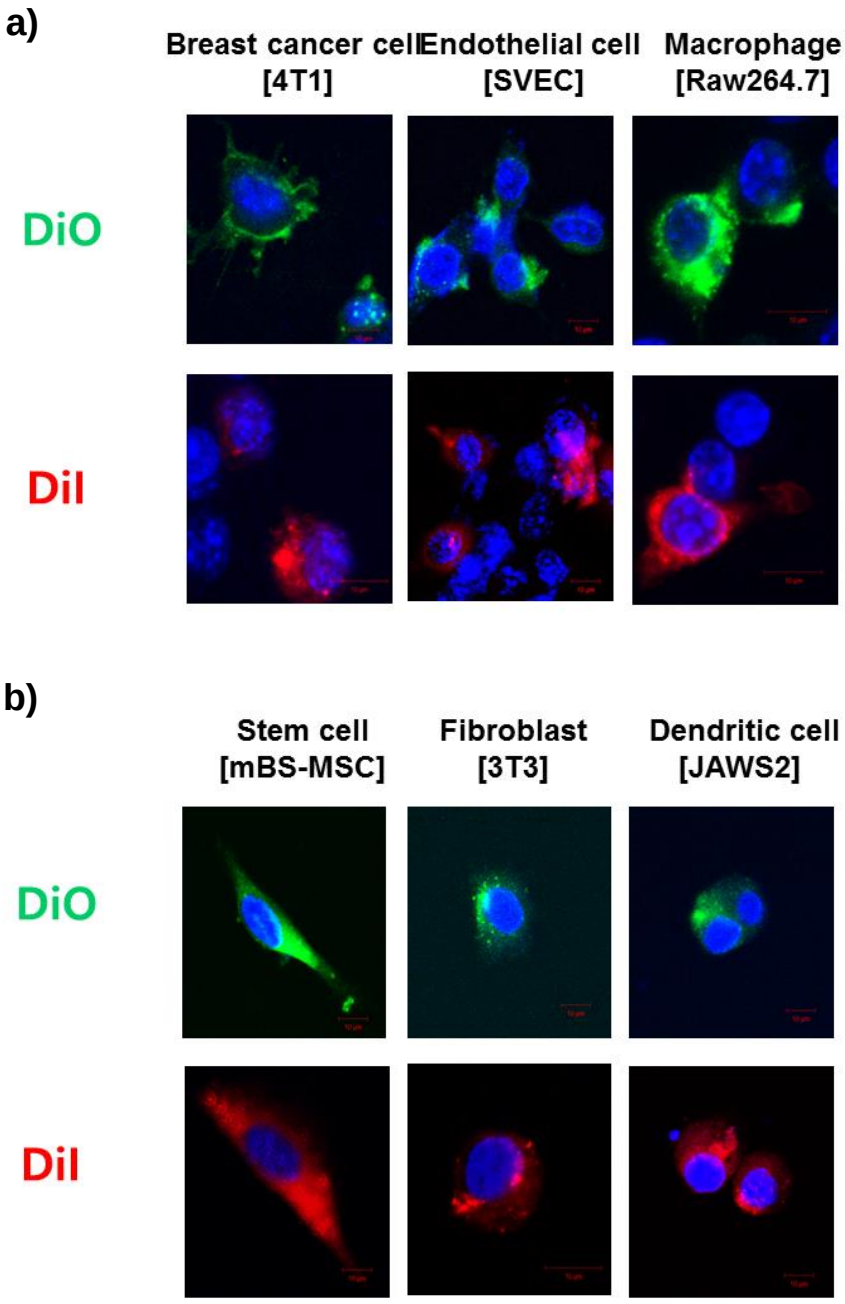

Figure 10. Exosome uptake images in tumor microenvironment cells.

In confocal microscopy, these fluorescently labeled exosomes were treated in various cells such as (a) tumor cells; 4T1, endothelial cells; SVEC, macrophage; Raw264.7, (b) stem cells; mBM-MSC, fibroblast; 3T3, and dentritic cells; JAWS2.

***In vitro* and i*n vivo* imaging of miR-210 activation in recipient cancer cells induced by exosomes from hypoxic cancer cells.**

To assess miR-210 transfer through hypoxic exosomes (Fig. 11a), 4T1-luc2/miR-210 cells and SVEC-luc2/miR-210 cells were constructed with a signal-off system vector, in which luciferase signals could be turned off by binding to miR-210 (Fig. 11b). The experimental scheme is illustrated in Fig. 11c. To obtain hypoxic exosomes from 4T1 cell, DFO (400 μM) was added to 4T1 cells for 48 h. These exosomes were treated *in vitro* and *in vivo*. To confirm miR-210 transfer *in vitro*, 4T1-luc2/miR-210 cells (Fig. 12a and 12b) and SVEC-luc2/miR-210 cells (Fig. 13a and 13b) were treated with different concentrations (0, 200, 400, 800 μg/mL) of hypoxic exosomes, and evaluated using bioluminescence imaging and luciferase assay. IVIS images showed that the luciferase signals in 4T1-luc2/miR-210 cells and SVEC-luc2/miR-210 cells decreased in a dose dependent manner. Luciferase assay also showed a dose dependent decrease in luciferase activity (Fig. 12c and 13c). Wound healing assays showed that migration of Exo (+) SVEC cells was higher than Exo (-) SVEC cells (Fig. 14a), and capillary-like structures increased in Exo (+) SVEC cells (Fig. 14b).

In bioluminescence imaging of cells at 48 h after exosome treatment (400 μg/mL), luciferase signals of Exo (+) 4T1 cells were lesser than those of Exo (-)

4T1 cells (Fig. 15a). From ROIs of Exo (-) 4T1 cells and Exo (+) 4T1 cells, signals of Exo (+) 4T1 cells decreased significantly, 0.67±0.12 fold, as compared to those of Exo (-) 4T1 cells (P = 0. 0262). In bioluminescence imaging of xenograft models (Fig. 15b), luciferase signals of Exo (+) tumor also decreased after exosome treatment, while signals of Exo (-) tumor remained consistent before and after treatment. From ROIs, signals of Exo (+) tumor were significantly decreased, by 0.56±0.12 fold (p = 0. 0174), whereas signals of Exo (-) tumor did not decrease significantly. In tissues (Fig. 16), luciferase expression in Exo (+) tumor was decreased, as compared to that in Exo (-) tumor. Expression of Ephrin-A3 and PTP1B, which are miR-210 target proteins, also decreased in Exo (+) tumor, as compared to that in Exo (-) tumor. However, VEGF expression was increased in Exo (+) tumor, as compared to that in Exo (-) tumor. Fig. 17 shows the western blot analysis from FFPE tissues, which has similar results to IHC. Ephrin-A3 and PTP1B expressions decreased in Exo (+) tumors, while VEGF increased in Exo (+) tumors.

In summary (Fig. 18), hypoxic tumor cells release miR-210-overexpressed exosomes and affect recipient cells. In this study, transfer of miR-210 through exosomes was successfully visualized in luciferase signal-off imaging, resulting in inhibition of miR-210 target genes, such as Ephrin-A3 and PTP1B.

This result showed that angiogenesis-related genes were inhibited through transfer of hypoxic exosomes, and that exosomes could affect VEGF and VEGF mediated EC recruitment.

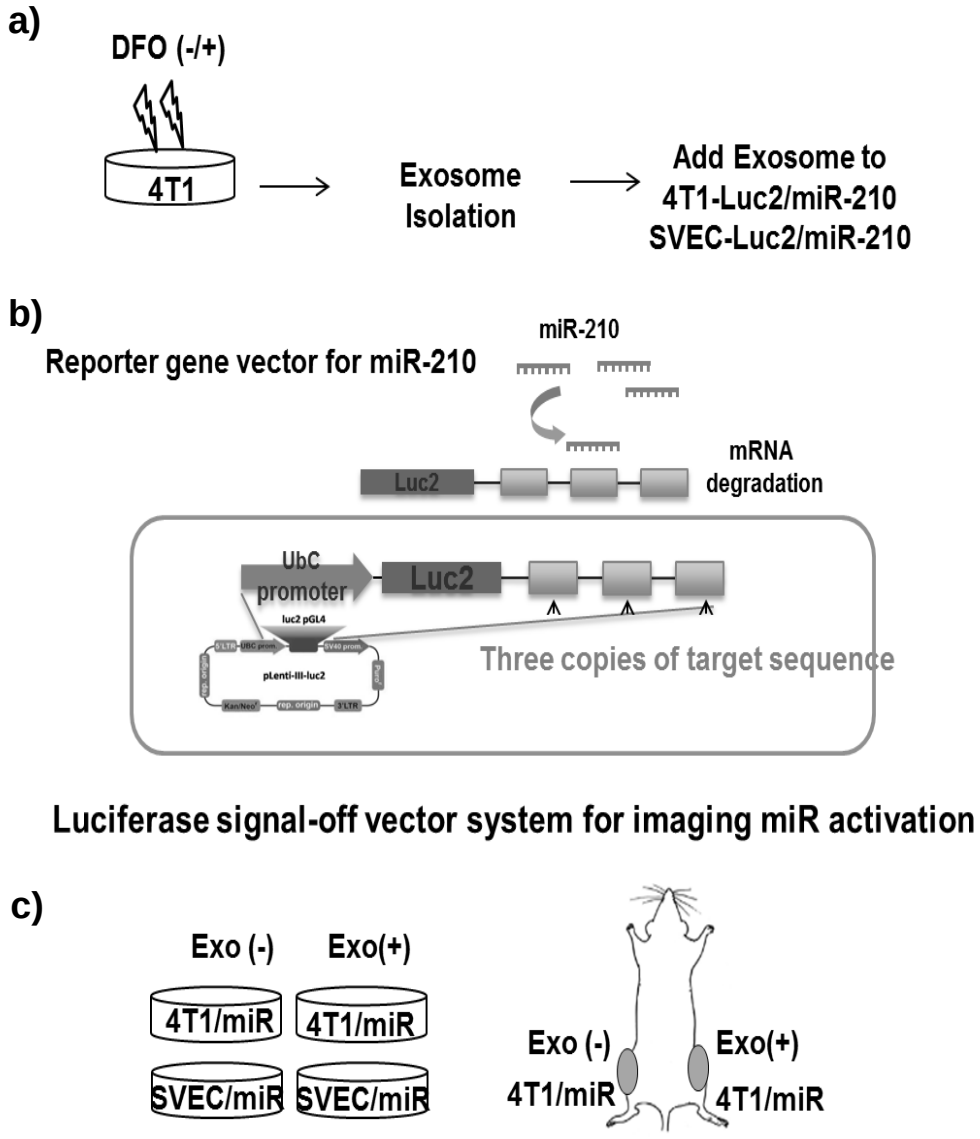

Figure 11. Schematic of the experimental scheme.

To image miR-210 activation induced by (a) hypoxic exosomes, 4T1 cells and SVEC cells were transfected with (b) a luciferase signal-off vector to image miR-210. (c) The experimental scheme is illustrated.

a)

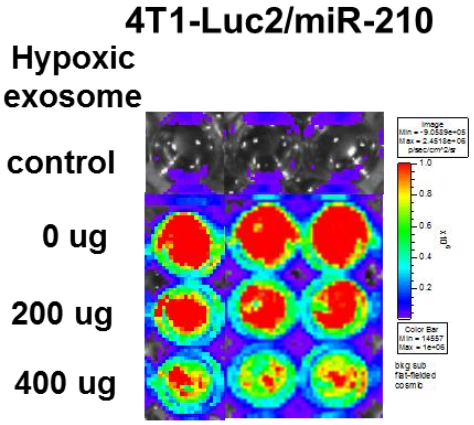
4T1-Luc2/miR-210
Hypoxic exosome
control
0 ug
200 ug
400 ug

b)

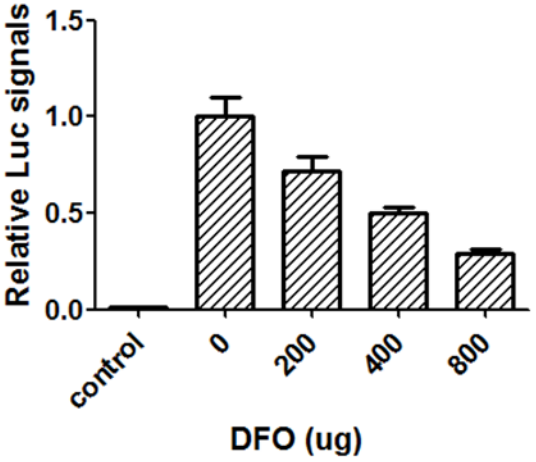
Relative Luc signals
1.5
1.0
0.5
0.0
control
0
200
400
800
DFO (ug)

c)

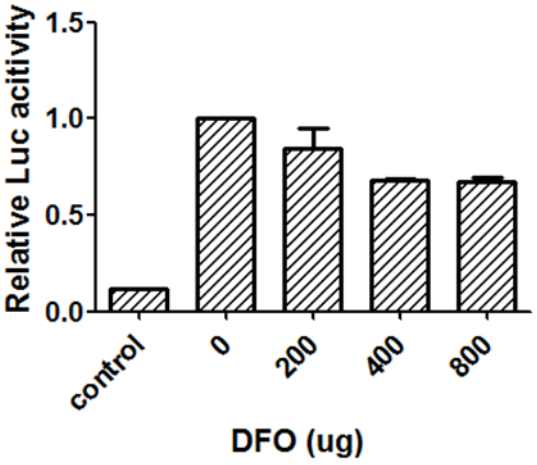
Relative Luc acitivity
1.5
1.0
0.5
0.0
control
0
200
400
800
DFO (ug)

Figure 12. Imaging for miR-210 activation by hypoxic exosomes in 4T1 cells.

Hypoxic exosomes were added in a dose-dependent manner (0, 200, 400, 800 μg/mL) to 4T1 cells, and (a and b) IVIS images showed that the luciferase signals in 4T1 cells decreased in a dose-dependent manner. (c) The luciferase assay also showed a dose-dependent decrease in luciferase activity.

a)

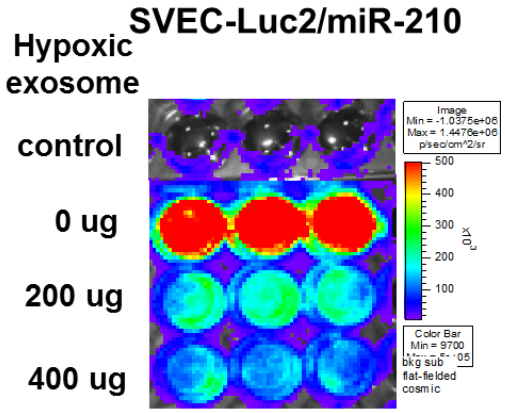
SVEC-Luc2/miR-210
Hypoxic exosome
control
0 ug
200 ug
400 ug
Image
Min = -1.0375e+06
Max = 1.4476e+06
p/sec/cm^2/sr
500
400
300
200
100
x10^3
Color Bar
Min = 9700
bkg sub
flat-fielded
cosmic

b)

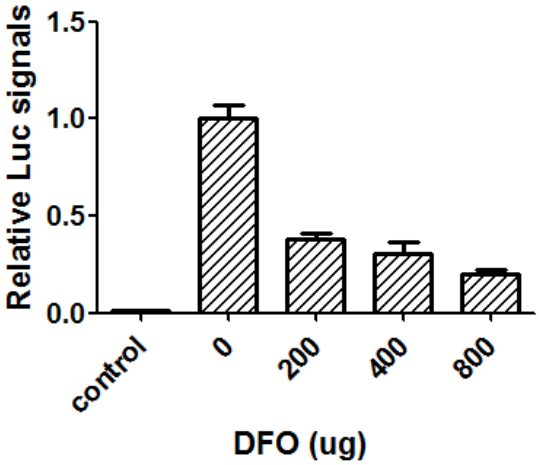
Relative Luc signals
1.5
1.0
0.5
0.0
control
0
200
400
800
DFO (ug)

c)

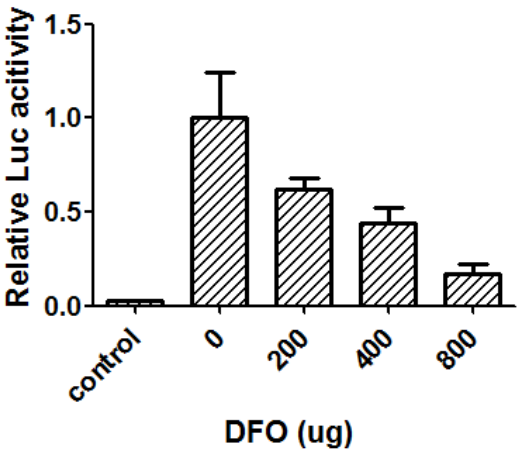
Relative Luc acitivity
1.5
1.0
0.5
0.0
control
0
200
400
800
DFO (ug)

Figure 13. Imaging for miR-210 activation by hypoxic exosomes in SVEC cells.

Hypoxic exosomes were added in a dose-dependent manner (0, 200, 400, 800 μg/mL) to SVEC cells, and (a and b) IVIS images showed that the luciferase signals in SVEC cells decreased in a dose-dependent manner. (c) The luciferase assay also showed a dose-dependent decrease in luciferase activity.

a) **Wound healing assay**

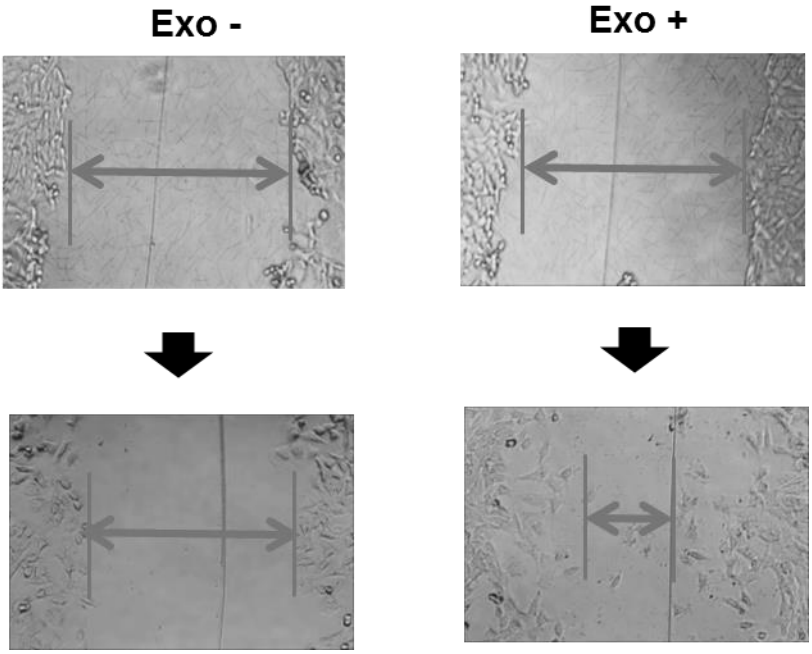

b) **Capillary like structure**

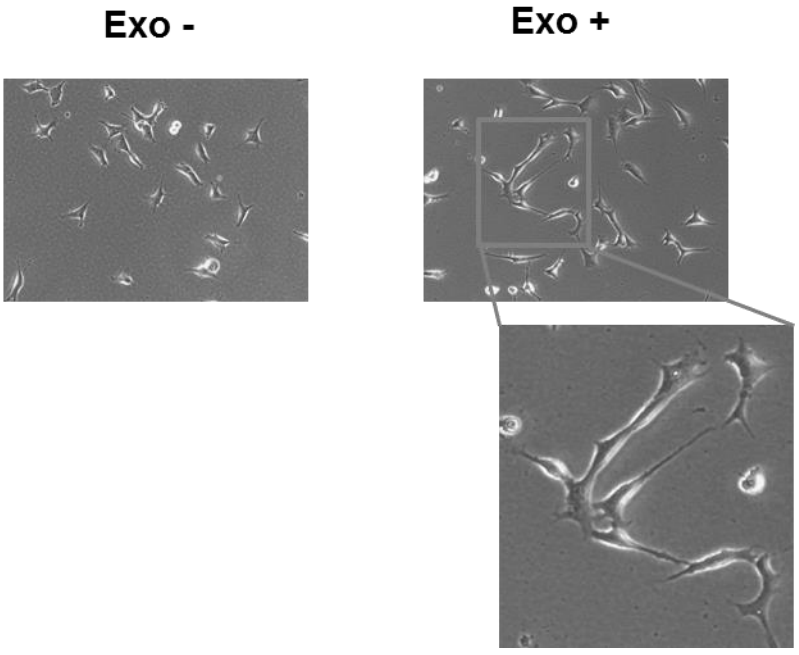

Figure 14. Wound healing assay and capillary-like structure in hypoxic exosomes treated SVEC cells.

(a) Wound healing assays showed that migration of Exo (+) SVEC cells was higher than Exo (-) SVEC cells, and (b) capillary-like structure was also enhanced in Exo (+) SVEC cells.

a)

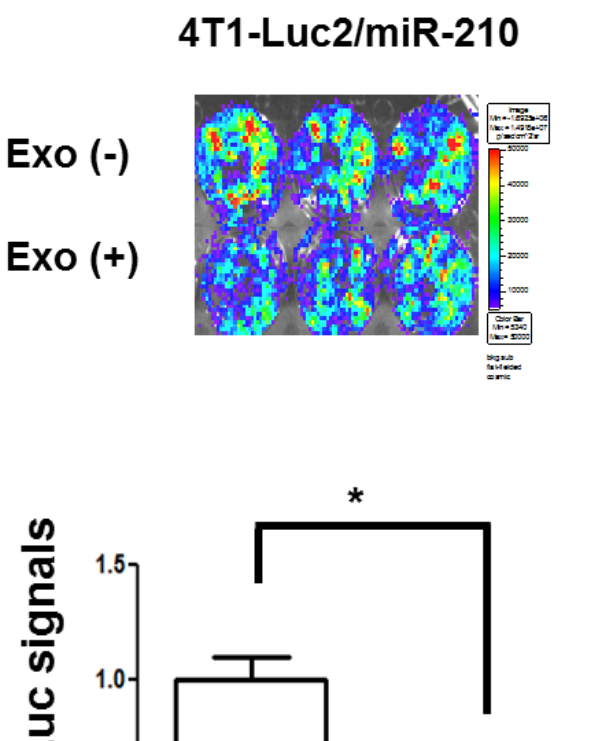
4T1-Luc2/miR-210
Exo (-)
Exo (+)
*
Relative Luc signals
1.5
1.0
0.5
0.0
Exo(-)
Exo(+)

b)

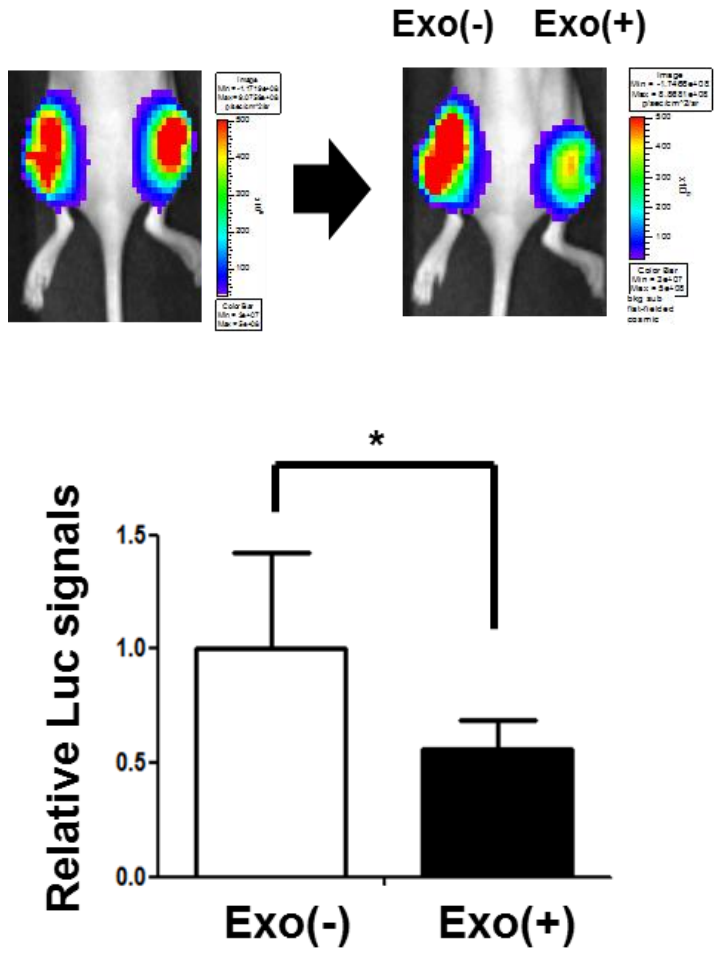

Figure 15. Imaging for miR-210 activation after hypoxic exosome treatment in cells and animal models.

(a) In bioluminescence imaging of cells at 48 h after exosome treatment (400 μg/mL), luciferase signals of Exo (+) 4T1 cells were significantly decreased (0.67±0.12 fold), compared to those of Exo (-) 4T1 cells under same conditions. Hypoxic exosomes were treated by intratumoral injection for *in vivo* studies. (b)

The signals of Exo (+) tumors were significantly decreased (0.56±0.12 fold) 48 h after exosome treatment, while signals of Exo (-) tumors did not decrease significantly (n = 4). *statistical significance with p values <0.05.

Changes of protein expression

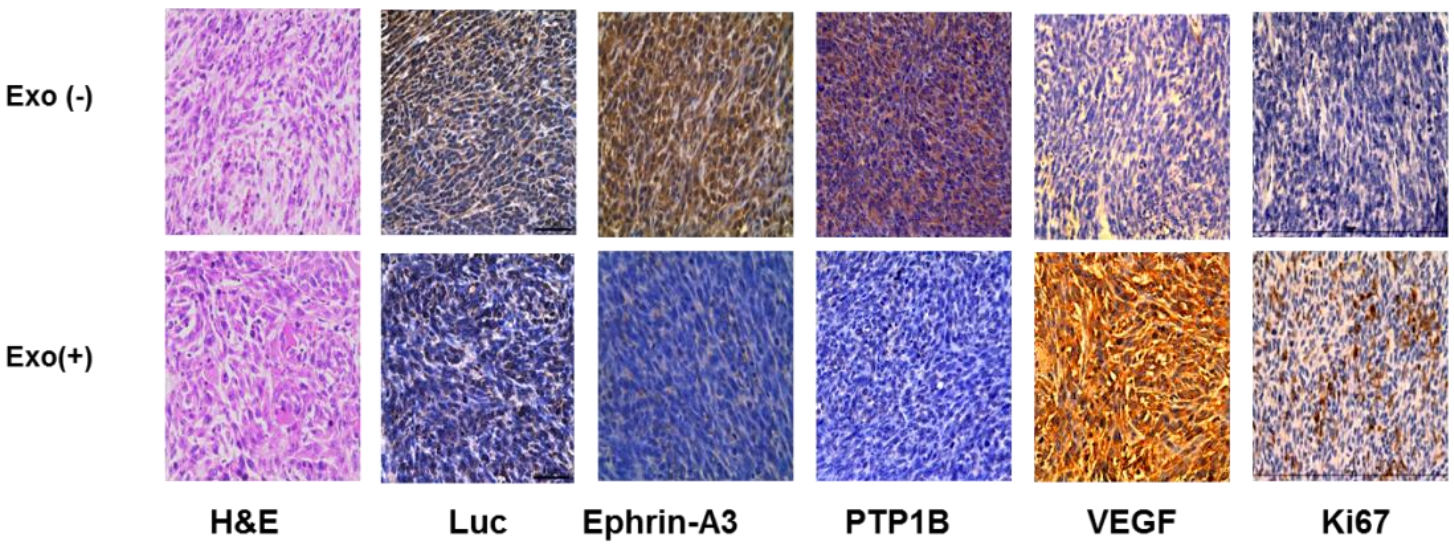

Figure 16. *Ex vivo* studies for miR-210 activation after hypoxic exosome treatment.

In tissues, the expression of luciferase and miR-210 targets, Ephrin-A3 and PTP1B, in Exo (+) tumors decreased compared to that in Exo (-) tumors, while expression of VEGF increased in Exo (+) tumors.

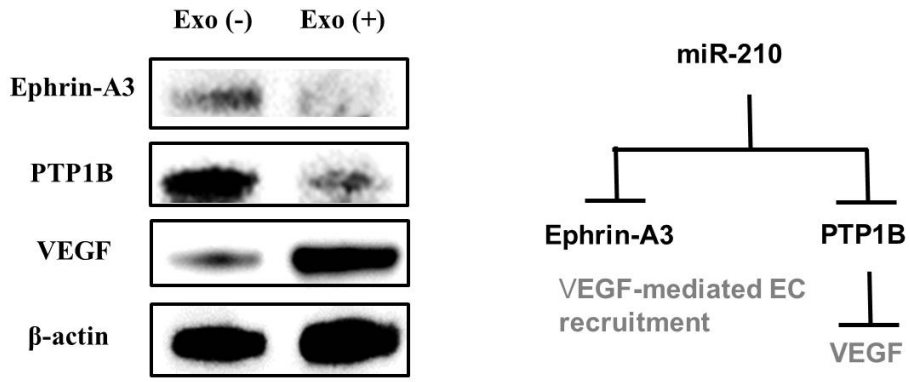

Figure 17. Effects of hypoxic exosomes in FFPE tissues.

Western blotting from FFPE tissues showed that the results were similar to those of IHC analysis.

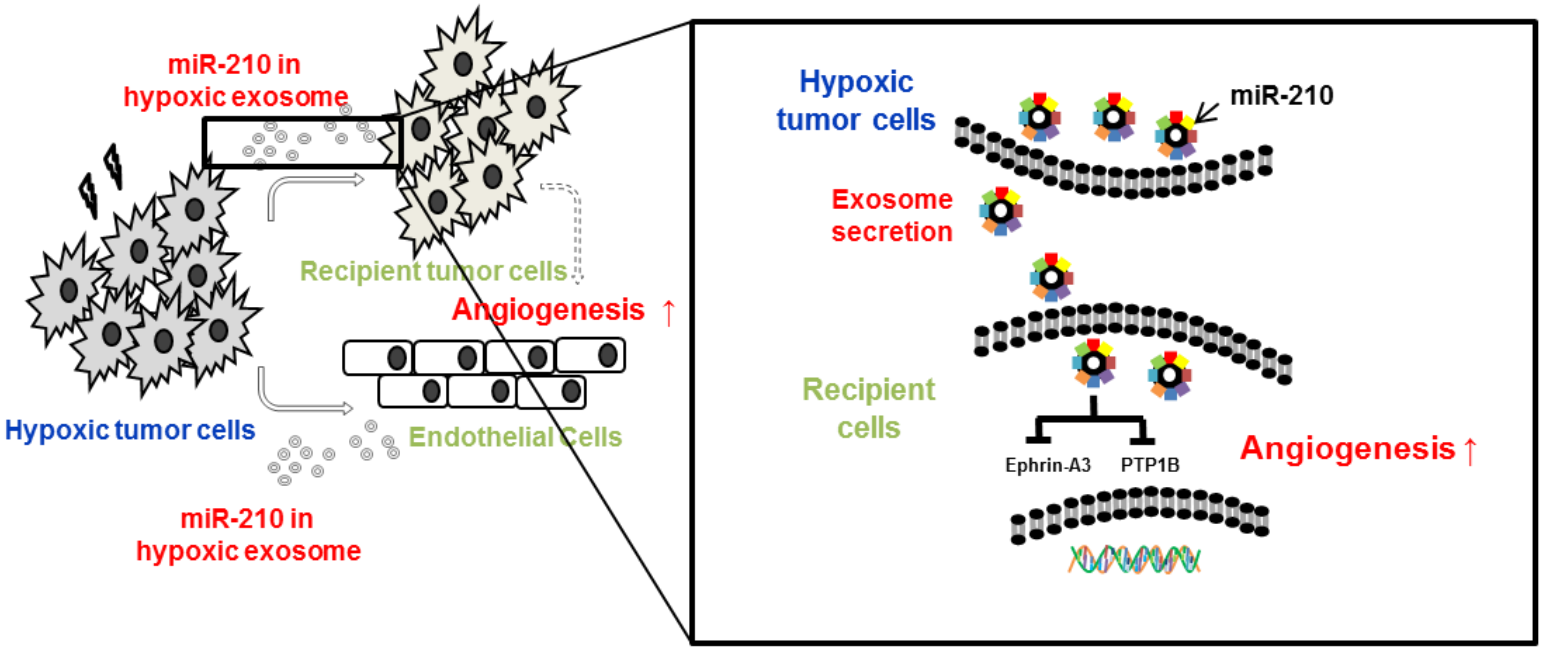

miR-210	3’ AGUCGGCGACAGUGUGCGUGUC 5’
EFNA3 3’UTR	5’ ACAGGACCUAUGCAACGCACAG 3’
PTP1B 537-542	5’ AGGTTCGTTAAAATGCGCACAA 3’

Figure 18. Summary.

Hypoxic tumor cells release exosomal miR-210 and affect the recipient cells: the surrounding tumor cells and endothelial cells. The recipient cells showed inhibition of miR-210 target genes such as Ephrin-A3 and PTP1B, which are angiogenesis-related genes.

DISCUSSION

In this study, we developed a reporter gene signal-off imaging system, using luciferase to monitor miR-210. We demonstrated that exosomes from hypoxic tumor cells transferred miRNA-210 to normoxic tumor cells and endothelial cells, and this exosomal miR-210 inhibited angiogenesis-related genes in recipient cells.

Cellular communication regulates basic cellular activities and coordinates functions (26). Cells can communicate with other cells via direct contact involving juxtacrine signaling; over short distances, involving paracrine signaling; or over long distances, involving endocrine signaling (27,28). Examples for direct contact include Notch signaling (29); for indirect contact, the communication is mediated by diffusible factors such as cytokines, hormones, and signaling molecules (30). Recently, exosomes have been actively investigated as novel messengers for cell-to-cell communication, because exosomes have many functional proteins, mRNAs, and miRNAs. The lipid bilayer of exosomes ensures the stability of their contents by protecting them from degradation by circulating proteases and nucleases (31-33).

The use of exosomes for diagnostic and therapeutic applications has received considerable attention (34, 35). Our data showed that fluorescence images in xenograft mouse models showed uptake of exosomes in tumors, suggesting

tumor tropism of exosomes (Fig. 5). Since they are bioavailable microvehicles that are well-tolerated, targetable to specific tissues, and membrane-permeable, exosomes make ideal candidates to deliver miRNA, proteins, drugs, and other molecules. In addition, exosomes have been highly investigated as cancer biomarkers (36). Our data also showed that exosomes of hypoxic tumor mouse serum have high levels of miR-210 compared to those of normal mouse serum (Fig.4). These results mean that miR-210 from exosomes in the mouse serum is a potential biomarker for hypoxic tumors.

Hypoxia is an important feature in tumors, and is related to malignant phenotypes and a poor prognosis in cancer patients (37,38). These hypoxic tumors may communicate with other tumors and surrounding non-tumor cells through exosomes. In particular, miR-210, which can be found in exosomes, and is induced by hypoxia, is associated with tumor progression, angiogenesis, and metastasis (39). There are many target genes of miR-210 such as Ephrin-A3, PTP1B, HOXA1, and FGFRL1. In our study, we selected Ephrin-A3 and PTP1B as our miR-210 targets because miR-210-overexpressed cells induced the downregulation of Ephrin-A3 and PTP1B. Ephrin-A3 is a receptor tyrosine kinase ligand, and PTP1B is a protein tyrosine phosphatase of the tyrosine phosphatase superfamily (40). Recently, it has been reported that Ephrin-A3 and PTP1B are related with crucial functions in

VEGF signaling and angiogenesis (41). Our results showed that expression of Ephrin-A3 and PTP1B in hypoxic exosome-treated tumors decreased through exosomal miR-210, increasing VEGF expression (Fig. 12). Diverse studies showed that Ephrin-A3 and PTP1B play important roles in the development of vascular remodeling (42). Our results indicate that downregulation of Ephrin-A3 and PTP1B by exosomal miR-210 modulates angiogenesis, resulting in angiogenic sprouting of capillaries and tubular structures.

Our results also showed that exosomal miR-210 from hypoxic cancer cells could affect recipient cancer cells, such as tumor cells and endothelial cells. However, there are additional cells in the tumor microenvironment (43), such as epithelial cells, immune cells, and mesenchymal stem cells (Fig. 10). It is possible that miRNAs in exosomes in cancer cells can be transferred not only to the surrounding cancer cells but also to neighboring stromal cells. The mode, effect, and clinical significances of exosome transfer to these microenvironment cells should be clarified. Another factor that must be taken into account is that exosome-mediated miR-210 functional efficiency is different in cell types. In our experiment, the same amount of exosomes was added to 4T1 cells and SVEC cells (Fig. 9,10). However, the luciferase signals of Exo (+) 4T1 cells significantly decreased, by 0.67-fold, whereas the luciferase signals of Exo (+) SVEC cells significantly

decreased, but only by 0.27-fold. These results suggest that efficiency of exosome-mediated miR-210 functionality is cell type dependent.

The transfer of hypoxic malignant phenotypes to normoxic cancer cells would have a great impact on the basic research and clinical applications in oncology (35, 36). It is well known that hypoxia induces a resistance to chemotherapy and radiotherapy, resulting in a poor prognosis (44-46). Modifications in therapy modalities have been investigated (47). One example is intensity-modulated radiation therapy (IMRT), which enables an optimized increase in dose to hypoxic tissues, leading to an improvement of therapy outcome (48, 49). In this study, we found that a hypoxic malignant phenotype of cancer cells can spread to adjacent cancer cells. This is important in identifying the region of real-time hypoxia in IMRT application.

However, little is known about the mechanism and role of exosomes in the progress of hypoxic phenotypes in malignant tumors. Transfer of miR-210 is just one mechanism in hypoxia development. Exosomes in hypoxic conditions could affect surrounding cells, and hypoxic responses could be mediated by other exosomal miRNAs, for example miR-31 and miR-424, which are also induced by hypoxia (50, 51). Further investigations are required for understanding the role of exosomal miRNAs in hypoxic signaling.

REFERENCES

1. Hanahan D, Weinberg RA. Hallmarks of Cancer: The Next Generation. *Cell.* 2011;144(5):646-74.

2. Ruan K, Song G, Ouyang G. Role of hypoxia in the hallmarks of human cancer. *J Cell Biochem*. 2009;107(6):1053-62.

3. Iyer NV, Kotch LE, Agani F, et al. Cellular and developmental control of O2 homeostasis by hypoxia-inducible factor 1 alpha. *Genes Dev.* 1998;12(2):149-62.

4. Semenza GL. Targeting HIF-1 for cancer therapy. *Nat Rev Cancer.* 2003;3(10):721-32.

5. Mees G, Dierckx R, Vangestel C, et al. Molecular imaging of hypoxia with radiolabelled agents. *Eur J Nucl Med Mol Imaging*. 2009;36(10):1674-86.

6. Krohn KA, Link JM, Mason RP. Molecular imaging of hypoxia. *J Nucl Med*. 2008;49 Suppl 2:129S-48S.

7. Wittmann J, Jack HM. Serum microRNAs as powerful cancer biomarkers. *Biochim Biophys Acta*. 2010;1806(2):200-7.

8. Iorio MV, Croce CM. MicroRNA dysregulation in cancer: diagnostics, monitoring and therapeutics. *EMBO Mol Med*. 2012;4(3):143-59.

9. Mathew LK, Simon MC. mir-210: a sensor for hypoxic stress during tumorigenesis. *Mol Cell*. 2009;35(6):737-8.

10. Huang X, Le QT, Giaccia AJ. MiR-210--micromanager of the hypoxia pathway. *Trends Mol Med*. 2010;16(5):230-7.

11. Alaiti MA, Ishikawa M, Masuda H, et al. Up-regulation of miR-210 by vascular endothelial growth factor in ex vivo expanded CD34+ cells

enhances cell-mediated angiogenesis. *J Cell Mol Med.* 2012;16(10):2413-21.

12. Cao X, Pfaff SL, Gage FH. A functional study of miR-124 in developing neural tube. *Genes Dev*. 2007;21:531–6.

13. Deo M, Yu JY, Chung KH, et al. Detection of mammalian microRNA expression by in situ hybridization with RNA oligonucleotides. *Dev. Dyn*. 2006;235:2538–48.

14. Ko HY, Hwang DW, Lee DS, et al. A reporter gene imaging system for monitoring microRNA biogenesis. *Nat Protoc*. 2009;4(11):1663-9.

15. Blasberg RG, Gelovani-Tjuvajev J. In vivo molecular-genetic imaging. J Cell Biochem Suppl. 2002;39:172-83.

16. Kang JH, Chung JK. Molecular-genetic imaging based on reporter gene expression. J Nucl Med. 2008;49:164S-79S..

17. Youn H, Chung JK. Reporter gene imaging. AJR Am J Roentgenol. 2013;201(2):206-14.

18. Ray P, De A. Reporter gene imaging in therapy and diagnosis. Theranostics. 2012; 2(4):333-4.

19. Thery C, Zitvogel L, Amigorena S. Exosomes: composition, biogenesis and function. *Nat Rev Immunol*. 2002;2(8):569-79.

20. Raposo G, Stoorvogel W. Extracellular vesicles: exosomes, microvesicles, and friends. *Cell Biol*. 2013;200: 373-83.

21. Quail DF, Joyce JA. Microenvironmental regulation of tumor progression and metastasis. *Nat. Med*. 2013;19**:**1423-37.

22. Record M, Subra C, Silvente-Poirot S, et al. Exosomes as intercellular signalosomes and pharmacological effectors. *Biochem. Pharmacol*. 2011;81: 1171-82.

23. Hannafon BN, Ding WQ. Intercellular Communication by Exosome-Derived microRNAs in Cancer. *Int. J. Mol. Sci*. 2013;14(7):14240-69.

24. King HW, Michael MZ, Gleadle JM. Hypoxic enhancement of exosome release by breast cancer cells. *BMC Cancer*. 2012;12:421.

25. Ho AS, Huang X, Cao H, et al. Circulating miR-210 as a Novel Hypoxia Marker in Pancreatic Cancer. *Transl Oncol*. 2010;3(2):109-13.

26. Koehler GA. Cellular communication. *Emergency medical services*. 1990;19(9):13-4.

27. Puente Vazquez J, Grande Pulido E, Anton Aparicio LM. Cytokine and endocrine signaling in prostate cancer. *Med Oncol*. 2012;29(3):1956-63.

28. Singh AB, Harris RC. Autocrine, paracrine and juxtacrine signaling by EGFR ligands. *Cell Signal*. 2005;17(10):1183-93.

29. Lewis J. Notch signalling and the control of cell fate choices in vertebrates. Semin *Cell Dev Biol*. 1998;9(6):583-9.

30. Scott WJ, Jr., Schreiner CM, Goetz JA, et al. Cadmium-induced postaxial forelimb ectrodactyly: association with altered sonic hedgehog signaling. *Reprod Toxicol*. 2005;19(4):479-85.

31. Chou J, Shahi P, Werb Z. microRNA-mediated regulation of the tumor microenvironment. *Cell Cycle*. 2013;12(20):3262-71.

32. Ochiya T, Lotvall J. Exosome as a novel shuttle for innovation. Preface. *Adv Drug Deliv Rev*. 2013;65(3):v.

33. Umezu T, Ohyashiki K, Kuroda M, et al. Leukemia cell to endothelial cell communication via exosomal miRNAs. *Oncogene*. 2013;32(22):2747-55.

34. Tickner JA, Urquhart AJ, Stephenson SA, et al. Functions and therapeutic roles of exosomes in cancer. *Front. Oncol*. 2014;4:127.

35. Tan A, Rajadas J, Seifalian AM. Exosomes as nano-theranostic delivery platforms for gene therapy. *Adv Drug Deliver Rev*. 2013;65(3):357-67.

36. Lasser C. Exosomal RNA as biomarkers and the therapeutic potential of exosome vectors. *Expert Opin Biol Ther*. 2012;12 Suppl 1:S189-97.

37. Arvelo F, Cotte C. Hypoxia in cancer malignity. *Invest Clin*, 2009;50:529-546.

38. Vaupel P, Mayer A. Hypoxia in cancer: significance and impact on clinical outcome. *Cancer Metastasis Rev*. 2007;26(2):225-39.

39. Dang K, Myers KA. The role of hypoxia-induced miR-210 in cancer progression. *Int J Mol Sci* 2015;16:6353-6372.

40. Fasanaro P, D'Alessandra Y, Di Stefano V, et al. MicroRNA-210 modulates endothelial cell response to hypoxia and inhibits the receptor tyrosine kinase ligand Ephrin-A3. *J Biol Chem*. 2008;283(23):15878-83.

41. Gee HE, Ivan C, Calin GA, et al. HypoxamiRs and cancer: from biology to targeted therapy. *Antioxid Redox Sign.* 2014;21:1220-1238.

42. Kuijper S, Turner CJ, Adams RH. Regulation of angiogenesis by Eph-ephrin interactions. *Trends Cardiovasc Med*. 2007;17(5):145-51.

43. Catalano V, Turdo A, Di Franco S, et al. Tumor and its microenvironment: A synergistic interplay. Semin *Cancer Biol*. 2013.

44. Wilson WR, Hay MP. Targeting hypoxia in cancer therapy. *Nat Rev Cancer*. 2011;11(6):393-410.

45. Harada H. How can we overcome tumor hypoxia in radiation therapy? *J Radiat Res*. 2011;52(5):545-56.

46. Rhim T, Lee DY, Lee M. Hypoxia as a target for tissue specific gene therapy. *J. Control Release*. 2013;172(2):484-94.

47. Geets X, Gregoire V, Lee JA. Implementation of hypoxia PET imaging in radiation therapy planning. *Q J Nucl Med Mol Imaging*. 2013;57(3):271-82.

48. Lee NY, Le QT. New developments in radiation therapy for head and neck cancer: intensity-modulated radiation therapy and hypoxia targeting. *Semin Oncol*. 2008;35(3):236-50.

49. Askoxylakis V, Dinkel J, Eichinger M, et al. Multimodal hypoxia imaging and intensity modulated radiation therapy for unresectable non-small-cell lung cancer: the HIL trial. *Radiat Oncol*. 2012;7:157.

50. Ghosh G, Subramanian IV, Adhikari N, et al. Hypoxia-induced microRNA-424 expression in human endothelial cells regulates HIF-

alpha isoforms and promotes angiogenesis. *J Clin Invest*. 2010;120(11):4141-54.

51. Liu CJ, Tsai MM, Hung PS, et al. miR-31 ablates expression of the HIF regulatory factor FIH to activate the HIF pathway in head and neck carcinoma. *Cancer Res*. 2010;70(4):1635-44.

국문 초록

서론: 세포 사이의 정보전달을 하기 위해 세포는 단백질, mRNA, miRNA 와 같은 특정세포 구성물을 포함하고 있다고 알려진 엑소좀을 분비한다. 특히, 암세포는 엑소좀을 이용하여 종양미세환경의 다른 세포에 활발히 정보전달을 한다. 이 연구에서는 miR-210 의 기능을 영상화하기 위한 DNA 리포터 유전자 벡터를 구축했고, 이 벡터를 발현하는 세포주를 만들었다. 저산소의 암세포에 의해 유도된 엑소좀을 암세포와 내피세포에 처리하여 받는 세포에서의 miR-210 의 발현과 기능을 확인하였다.

재료 및 방법: miR-210 의 기능을 평가하기 위해, miR-210 이 결합되면 발광효소 신호가 감소가 되도록 만들어진 miR-210 특이적 리포터 유전자를 개발했다. 이러한 벡터를 이용하여 4T1 세포 (마우스 유방암세포)와 SVEC 세포 (내피세포)는 형질주입되었다. 저산소 상태는 DFO 에 의해 유도되었다. 저산소 상태의 엑소좀은 초원심분리기 또는 엑소퀵으로 분리되었고, 웨스턴 블롯과 전자현미경을 통해 확인했다. 실시간 중합효소 연쇄반응을 통해 miR-210 의 양은 측정되었다. 발광효소는 발광효소분석와 IVIS 영상을 통해 확인되었다. 종양조직에서는 HIF-1a, 발광효소,

Ephrin-A3, PTP1B, VEGF 의 발현이 면역조직화학 방법을 통해 확인 되었다.

결과: miR-210 은 저산소 세포에서는 증가하였고, 저산소 세포에서 분비된 엑소좀에서는 증가되었다. 생체발광영상에서는 저산소상태의 엑소좀을 처리한 4T1 과 SVEC 세포에서의 발광효소 신호가 감소하는 것을 확인할 수 있었다. 마우스모델에서는 저산소 상태의 엑소좀을 처리한 종양에서의 발광효소 신호가 엑소좀을 처리하지 않은 종양에 비해 감소하는 것을 볼 수 있었다. 이는 miR-210 이 엑소좀을 통해 이동하였다는 것을 보여준다. 저산소 상태의 엑소좀을 처리한 종양세포조직에서는 miR-210 타겟 단백질인 Ephrin-A3 와 PTP1B 이 감소한 반면, VEGF 는 증가한 것을 확인할 수 있었다.

결론: 저산소의 암세포에서 암세포와 내피세포로 엑소좀을 통한 miR-210 의 이동을 성공적으로 영상을 통해 확인하였고, 이는 혈관생성 관련 유전자에 영향을 주었다. 이러한 영상시스템은 종양미세환경의 다른 세포에서 엑소좀의 기본적인 메커니즘과 세포간의 신호전달을 이해하는데 적용될 수 있다.

주요어: 유방암, 엑소좀, 저산소, miR-210, 종양미세환경

학 번: 2010-23745